Myoung-Woon Moon[a,b], Seok Chung[c], Kwang-Ryeol Lee[b], Kyu Hwan Oh[d],
Howard A. Stone[a], John W. Hutchinson[a]

[a] School of Engineering and Applied Sciences, Harvard University, Cambridge, USA
[b] Future Fusion Technology Laboratory, Korea Institute of Science and Technology, Seoul, KOREA
[c] Biological Engineering Division, Massachusetts Institute of Technology, Cambridge MA, USA
[d] Department of Materials Science and Engineering, Seoul National University, Seoul, KOREA

Directed assembly of fluidic networks by buckle delamination of films on patterned substrates

Dedicated to Professor A. G. Evans on the occasion of his 65th birthday

A method to create networks of intricate fluidic channels formed from metals and ceramics is proposed and demonstrated. The method exploits buckle delamination of a thin compressed film bonded to a substrate. A low adhesion layer coinciding with the desired layout of the channel network is laid down prior to deposition of the film. Once triggered, the buckle delamination propagates along the low adhesion pathways driven by release of the elastic energy stored in the film, assembling the entire channel network without external intervention. Strips, tapered strips and a selection of grids are demonstrated for diamond-like carbon films bonded to Si substrates with gold providing low adhesion. Control of the film thickness (15 nm to 260 nm) and the width of the low adhesion regions (200 nm to microns) enables the cross-sectional area of the channel to be defined precisely with height determined by the buckle amplitude (40 nm to 500 nm). The channel network has been integrated with a microfluidic interface formed from poly-dimethylsiloxane. Pressure-driven flow of two miscible streams shows convectively enhanced mixing in these nanoscale buckled channels.

Keywords: Buckling delamination; Buckling patterning; Nanochannel; Fluidic channel

1. Introduction

Intriguing though they may be, buckling delaminations of thin films bonded to substrates are usually the undesirable consequence of some combination of overly high compressive film stress, films that are too thick, or poor interfacial adhesion. Films under compressive stress are susceptible to buckling delamination when the elastic energy per unit area stored in the film exceeds the energy per area required to decohere the interface [1–4]. The mechanics of buckling delamination has been studied for two decades [1–7] with emphasis on delamination avoidance. Recently, a way to harness buckling delamination for creating microchannels emerged from a study that systematically introduced inter-face regions of low adhesion [8]. The method entails controlling the path and width of the delamination by laying down on the substrate, prior to deposition of the film, a layer of a third material having low adhesion with the film and coinciding with the desired network of channels. For combinations of film stress and thickness chosen to decohere only the low adhesion regions, the delamination, once triggered, traverses the entire low adhesion pattern creating a network of channels with precisely formed cross-sections having sub-micron openings.

The system used to demonstrate the feasibility of the approach employs a silicon substrate, gold deposited in prescribed patterns by e-beam lithography as the low adhesion layer, and vapor deposited films of diamond-like-carbon (DLC). Films ranging in thickness from 15 nm to 260 nm have been deposited. The equi-biaxial compressive stress in the film is $\sigma_0 \cong 1\,\mathrm{GPa}$. The channel width is determined by the width of the low adhesion layer and was varied from 200 nm to tens of microns. The amplitude of the buckled film determines the opening of the channel; it ranges from tens to hundreds of nanometers.

Channel networks have been created with varying degrees of intricacy: straight strips (Fig. 1a); sequenced zig-zag channels (Fig. 1b); rectangular grids (Fig. 1c); and hexagonal grids (Fig. 1d). For the specific system, DLC film is well known for its electrical and mechanical properties such as electrical insulating capability and high elastic modulus [4, 8]. Furthermore, in addition to its potential biocompatibility and chemical inertness [9, 10], its wear resistance makes it attractive for prolonged lifetimes [10, 11] and its transparency allows visualization of flow within the channels. The gold layer is also attractive for its inertness in biological and chemical environments [12–14].

Guidelines derived from the mechanics of buckle delamination [1–8] are proposed for choosing the film thickness along with constraints on the adhesion energies to arrive at designs for specific channel widths and openings. Procedures used to create the present system are outlined in the methods section, including integration with a micro-interface with inlet and outlet ports, and a specific flow system is demonstrated.

M.-W. Moon et al.: Directed assembly of fluidic networks by buckle delamination of films on patterned substrates
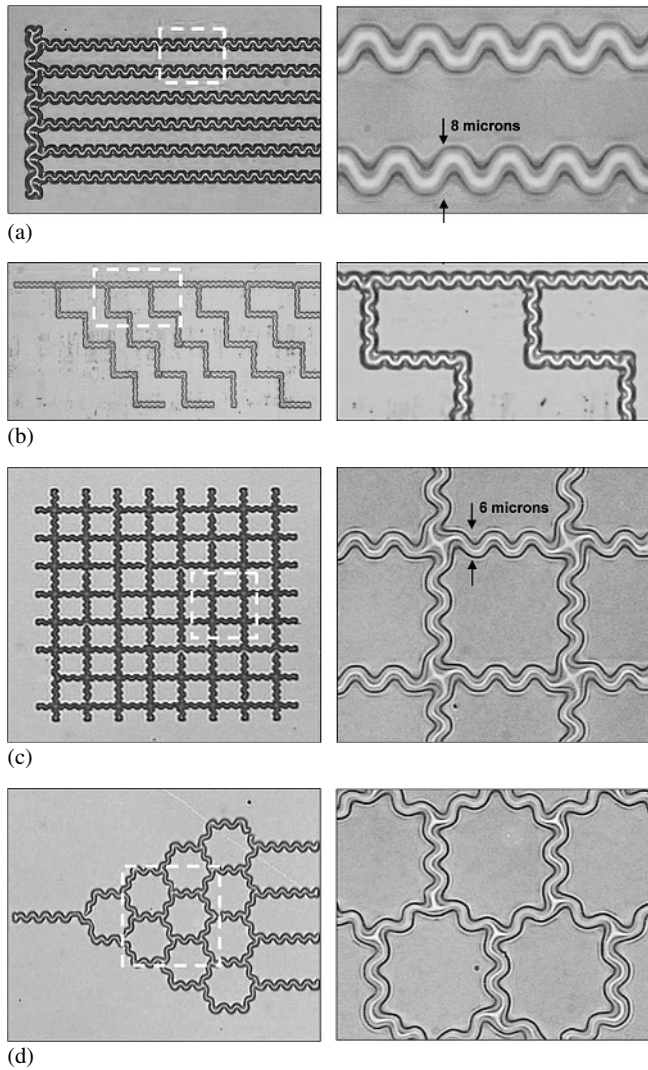

(a)

(b)

(c)

(d)

Fig. 1. Networks of channels of DLC films on Si substrates patterned using Au as the low adhesion layer, as viewed by optical microscopy. Amplified sections are shown on the right. In all these cases the width of the low adhesion strips is such that the telephone cord morphology forms.

2. Experimental procedure

The process for developing the micro-fluidic system is divided into two overall steps: creation of the buckling pattern array on substrate (Fig. 2a–d), and fabrication of the PDMS integration layer (Fig. 2e–h).

2.1. Channel network

Regions of an Au layer coinciding with the desired channel network were patterned onto Si substrates with e-beam lithography techniques in a clean room environment followed by DLC deposition [8]. A positive e-beam resist (ER) layer was spin-coated on Si (100) followed by e-beam exposure of the regions selected for low adhesion with resolution to 20 nm for the strip width. A thin layer of Au (2 ∼ 3 nm) was ion-coated over the patterned region, followed by removal with acetone and alcohol of the ER layer covering the regions designated for high adhesion. The DLC film was then deposited by the method of PECVD

(a) E-beam patterning

(b) Low adhesion layer deposition

(c) ER lift-off

(d) DLC deposition & buckling triggered

(e) Channel definition

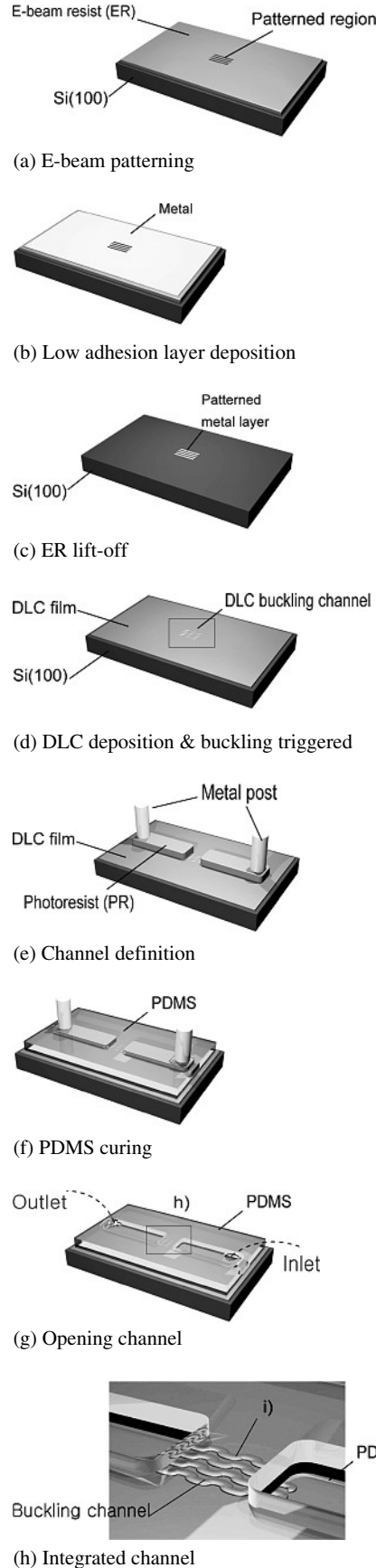(f) PDMS curing

(g) Opening channel

(h) Integrated channel

Fig. 2. Procedures for fabrication of the network of micro-channels and its integration with a connector package. Creation of the micro-channels in (a) to (d) using lithography methods and thin film deposition. Construction of PDMS integration package in (e) to (h) containing connector tunnels and millimeter-sized inlet and outlet holes.

using a capacitively-coupled r. f. glow discharge. Based on prior experience, deposition conditions can be set such that film characteristics such as modulus, thickness and pre-stress can be reproduced. The gas phases are C_6H_6, at a pressure of 133 Pa with deposition time ranging from several seconds to three minutes resulting in DLC film thickness of $15 \sim 260$ nm and resulting in a residual compression between about 0.9 and 1.5 GPa in the equi-baixial state [4, 8]. Buckle delaminations are triggered at a wide area of low adhesion laid down at one end of the channels (e. g. Fig. 1a), prodded by the AFM if necessary.

Although no direct observation of the location of the interface delamination crack was made, separation is believed to occur at the interface between the Au and the DLC due to the low adhesion between these materials. Film stresses and buckling geometries were determined using standard curvature measurement techniques and atomic force microscopy (AFM, AutoProbe CP Research sys.). Sections through the channel were made by using the Dual-Beam FIB (NOVA200, FEI Company).

2.2. Integration with a PDMS micro-interface

The second overall step stacks a PDMS layer [15 – 27] on the buckling channel array as depicted in Fig. 2e – h. Submillimeter-sized tunnels for conducting fluid to the fluidic network are laid down on top of the DLC using thick photo-resist (PR) lines which are subsequently dissolved away. Then, PDMS in a liquid state is poured on the DLC and PR lines. Metal "posts" of several millimeters in diameter are positioned at locations selected for inlet and outlet holes to the tunnels. The inlet hole can also serve as a storage "tank". The PDMS is cured; the posts are removed; and the PR is stripped away from the tunnels with acetone and ultrasonic stimulation. Stripping the PR also breaks a hole in the DLC film at the ends of the tunnels, creating the openings to the microfluidic network. The resulting PDMS layer has a thickness of 3 mm with good adherence to the DLC film. The geometry of the DLC channels does not appear to be altered by the PDMS, and it is likely the PDMS provides protection and extra support for the thin buckled DLC film, particularly at the film holes. For demonstration purposes, an integrated micro-chip (Fig. 3) was created with a network of parallel DLC channels and infiltrated with water as described above. A simple mixing experiment in a nanoscale opening channel was also demonstrated by stamping the buckling channel on PDMS (Fig. 3b). Pure water (right inlet) and fluorescent water (left inlet) were introduced on the two inlets in Fig. 3c. The fluorescent dyes (Fluorescein sodium, Aldrich chemical company inc. WI, USA). The fluorescent light intensity of green color was collected along the streamwise direction using an optical microscope equipped with a fluorescence ramp (EBQ 100). A channel 7.6 µm in width and 500 nm in maximum height was chosen and a flow speed 5 cm s^{-1} was achieved by controlled pressure.

3. Results and discussion

3.1. Dimensions of buckling channel

Denote the Young's modulus, Poisson ratio and thickness of the film by E, v and h, respectively, the half-width of

the channel by b, the in-plane bi-axial compressive stress in the unbuckled film by σ_0, the work/area of separation of the low and high adhesion interfaces by Γ_C and $\Gamma_C^{\text{substrate}}$, respectively.

A fundamental reference length is

$$b_0 = h \frac{\pi}{\sqrt{12(1 - v^2)}} \sqrt{\frac{E}{\sigma_0}} \qquad (1)$$

corresponding to the half-width of an infinitely long clamped plate subject to in-plane stress σ_0 at the *onset* of buckling [1–5]. The clamped plate model provides an excellent approximation to the behavior of the buckled film as long as the substrate is thick and its modulus is compar-
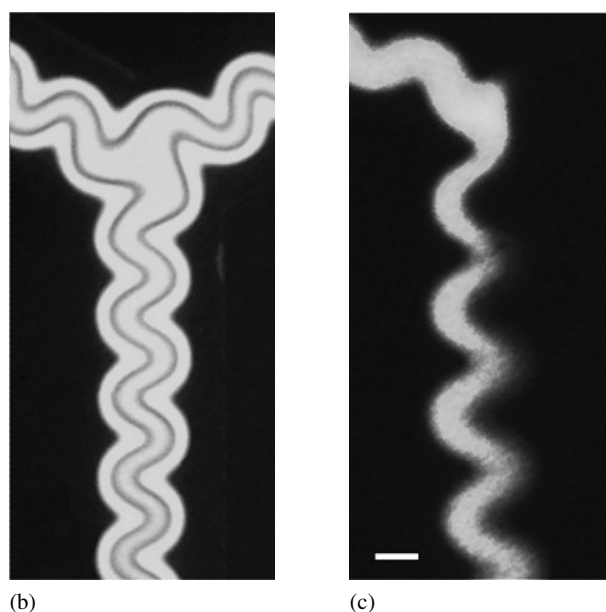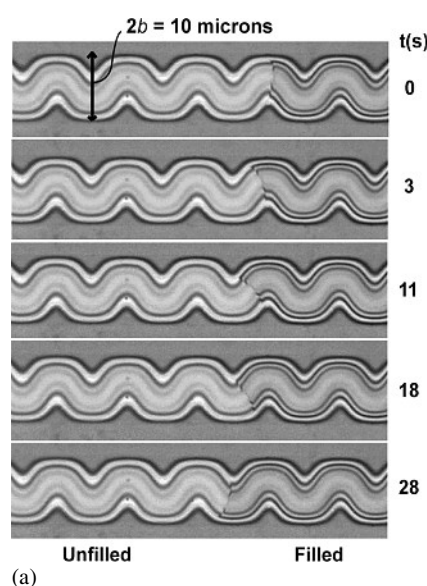

(a)

(b)   (c)

Fig. 3. (a) Sequence of images viewed through the transparent DLC film (120 nm thickness) of the front of a water column flowing through a telephone cord channel of width 10 µm and cross-sectional area 2.4 µm². (b) Mixing of two flows was performed using Y-shaped buckling channel stamped on PDMS. (c) The water with green fluorescent dyes (left) and the pure water (right) were joined at a junction. The length for complete mixing was measured as $l \sim 34$ µm. Channel size was 7.6 µm in width and 1.9 µm² in cross-section area. Bar = 5 µm.

able to that of the film [18]. Equally important is the elastic energy/area stored in the unbuckled film available subject to release under plane strain:

$$G_0 = \frac{\sigma_0^2 h}{2E(1 - \nu^2)} \qquad (2)$$

The two morphologies of the buckling mode revealed along the tapered strip in Fig. 4, the Euler mode (narrow region) and the telephone cord mode (wide region), depend on b/b_0 [3, 8]. For $\nu = 0.3$ (for DLC), the Euler mode exists for $1 < b/b_0 < 2.6$ while the telephone cord mode exists for $b/b_0 > 2.6$. For the Euler mode, the energy/area available to separate the interface averaged over the curved front of a delamination propagating under steady-state conditions is [1, 8]

$$G_{ss} = G_0 \left(1 - \left(\frac{b_0}{b} \right)^2 \right)^2 \qquad (3)$$

If $1 < b/b_0 < 2.6$, the condition for delaminating the low adhesion interface is

$$G_0 \left(1 - \left(\frac{b_0}{b} \right)^2 \right)^2 > \Gamma_C \qquad (4)$$

If $b/b_0 > 2.6$, such that telephone cord buckling occurs, G_{ss} is somewhat larger than the result in Eq. (3); to a good approximation, the requirement becomes $G_0 > \Gamma_C$ [8]. The delamination crack front imposes both tensile and shear stress intensities on the interface and, thus, the relevant interface energy, Γ_C, is that associated with the corresponding mix of intensities [4].

The condition that the delamination be contained by low adhesion strip requires that the energy release rate along the sides of the delamination, G_{side}, be less than $\Gamma_C^{substrate}$. G_{side} is larger than G_{ss} [2, 5]; it is adequately approximated for present purposes by $G_{side} \cong G_0$. Thus, $\Gamma_C^{substrate} \gg G_0$ ensures delamination will be confined to the low adhesion pathways.

A channel cross-section is photographed in Fig. 4a and depicted in Fig. 4b. The opening displacement of the Euler channel is $w = w_{max}(1 + \cos(\pi y/b))/2$, where y is measured from the center of the buckle, and

$$w_{max} = h \sqrt{\frac{4}{3} \left(\left(\frac{b}{b_0} \right)^2 - 1 \right)} \cong \frac{2hb}{\sqrt{3} b_0} \qquad (5)$$

The cross-sectional area of the channel is

$$A = \int_{-b}^{b} w \, \mathrm{d}y = b w_{max} \cong \frac{2hb^2}{\sqrt{3} b_0} \qquad (6)$$

The approximations in Eqs. (5) and (6) apply when $b > 2b_0$. They are strictly applicable only for $1 < b/b_0 < 2.6$, however they are approximately applicable for the telephone cord buckles [4].

A series of tapered low adhesion Au strips, such as that at the top of Fig. 4, were patterned with DLC films deposited on top under identical conditions to seven thicknesses ranging from 15 nm to 260 nm. The delamination propagates along the strip giving rise to the telephone cord morphology at the wide end and transitioning to the Euler mode as the strip narrows [8]. It arrests at the point where the strip width drops below the critical value in Eq. (4). Based the arrest data, the DLC/Au interface has $\Gamma_C \approx 0.1 \, \mathrm{J} \, \mathrm{m}^{-2}$. Measure-
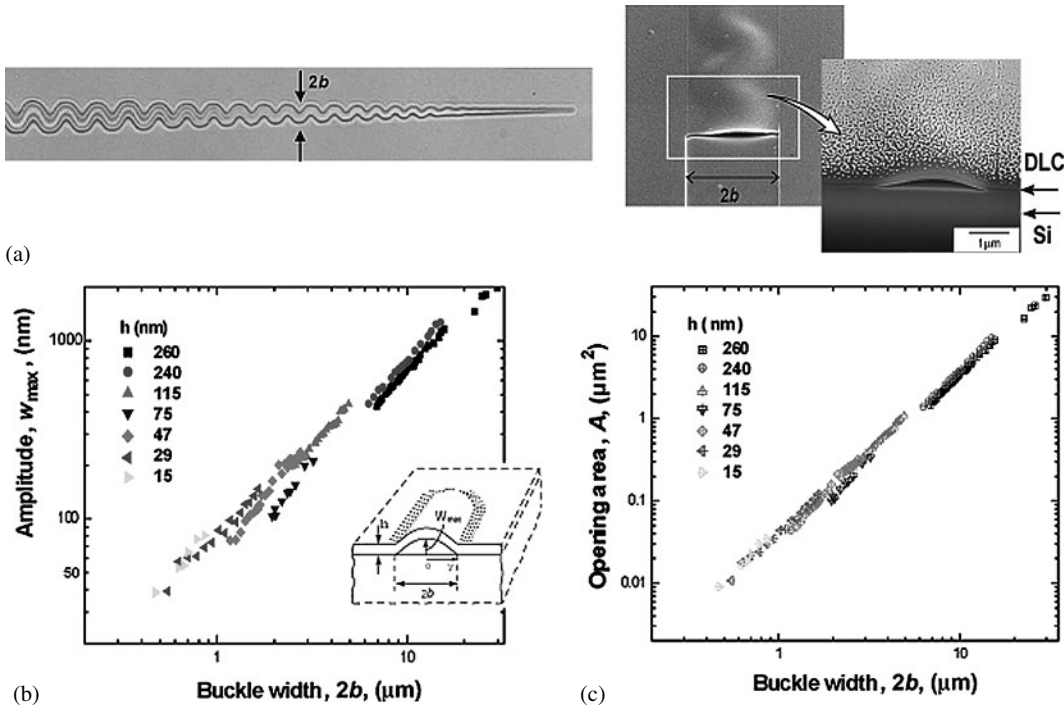

Fig. 4. (a) Delamination along a tapered low adhesion region. Cross-section of a channel cut with a focused ion beam viewed with a 52° tilting angle. The delamination buckle is triggered at the wide end and propagates toward the narrow end, arresting when the energy available to decohere the interface fails to satisfy Eq. (4). The telephone cord morphology at the wide end transitions to the Euler mode towards the narrow end. Tapered delaminations for seven film thicknesses were measured at locations along their length to generate data on (b) delamination amplitude and (c) delamination cross-sectional area.

ments for the DLC/Si interface indicate that $\Gamma_C^{\mathrm{substrate}}$ lies between 4 and 5 J m^{-2} [19].

The profile of the buckle was measured at numerous points along the strip using an AFM, providing the experimental points of maximum buckle height versus width plotted in Fig. 4b for each of the seven film thicknesses. The same data was used in connection with $A = bw_{\max}$ to plot the cross-sectional area of the channels versus channel width in Fig 4c. For each thickness except $h = 75$ nm, the data fall in the range such that $w_{\max} > 2h$ implying, from Eq. (5), that $b > 2b_0$. Thus, by Eqs. (5) and (6), it is expected that $w_{\max} \propto b$ and $A \propto b^2$ for each film thickness, as seen in Fig. 4. Moreover, by Eq. (1), $b_0 \propto h$, and thus it follows that $w_{\max}$ and A should be independent of h if $b > 2b_0$, as is indeed evident in Fig. 4. The only exception is the film with $h = 75$ nm where the smallest values of b are only slightly larger than b_0.

3.2. Fluidic channel application

At the scales relevant here, fluid can move through the channels driven by capillary action if hydrophilic conditions exist between the fluid and the channel walls [20–22]. With γ as the surface tension of fluid and θ_1 and θ_2 denoting its wetting angles with the film and the low adhesion layer, respectively, the pressure drop across the meniscus in a channel having uniform height, H, is $\Delta p = \gamma(\cos\theta_1 + \cos\theta_2)/H$. For laminar flow, the average fluid velocity due to this pressure drop along a channel of length L is $V = \Delta p H^2/(12\mu L)$ where μ is the fluid viscosity. If H is identified with the average opening of the channel, $w_{\max}/2$, then the flow in a channel open to the atmosphere at both ends with a meniscus at one end has [21–23]

$$V \cong \frac{\gamma(\cos\theta_1 + \cos\theta_2)\, w_{\max}}{24\mu L} \tag{7}$$

For water in channels of the size created here, Δp will generally exceed ten atmospheres assuming adequate wetting. The DLC and Au are hydrophilic with wetting angles of less than 70 degrees [24] and nearly zero [25–26], respectively.

Straight channels of telephone cord buckle delaminations of width 10 μm and length 1.5 mm were created with inlet and outlet ports in an integrated package (Fig. 2). De-ionized water was introduced at the channel inlet and a series of snap shots through the transparent DLC film (Fig. 3a) reveal the front of the fluid propagating along the channel. The front remains perpendicular to the centerline of the channel as the fluid moves through the channel. The velocity of the fluid can be controlled by adjusting the inlet and outlet pressures. When these pressures were atmospheric, velocities of the order of 10^{-3} m s^{-1} were observed, in accord with Eq. (7). To facilitate photography, the flow in Fig. 3a was slowed by controlling the outlet pressure.

In order to illustrate one use of these channels for manipulation or control of fluidic motions, we investigated fluid mixing. In particular, at a Y-shaped junction in a buckled channel (Fig. 3b) we combined a stream of pure water with fluorescently labeled water (Fig. 3c). The typical time for flow to convect through a length, L, along a channel is L/v, where v is the average velocity. The time to diffuse the width of the channel is b^2/D_{mol} [27, 28], where

D_{mol} is the molecular diffusion coefficient; $D_{\mathrm{mol}} = 3.0 \times 10^{-10}$ m^{2}s^{-1} for a fluorescence dye molecule. So under the assumption of purely diffusive mixing, we expect complete mixing over the cross-section of the channel when $L \sim \dfrac{b^2}{D_{\mathrm{mol}}} v \sim 2$ mm, for the channel with $b = 3.8$ μm, $v = 5$ cm s^{-1}, Our preliminary data is inconsistent with this prediction since for the flow in the channel in Fig. 3c, the length for complete mixing was measured as $L \sim 34$ μm, which suggests that flow enhancement mixing is occurring rather than diffusive mixing. These observations of convectively enhanced mixing are the subject of on-going work and will be reported in a future communication.

4. Conclusions.

In summary, we have reported a method, utilizing buckle delamination of thin films, for controlling the shape and connectivity of a network of nanoscale channels. Channel dimensions have been fabricated with cross sectional areas ranging from 10^{-2} μm^2 to 10 μm^2. The approach is useful for developing confined fluidic networks of precise channels for world-to-chip microfluidic devices [28–30]. As we have demonstrated, intricately arrayed networks can be assembled with channels of varying dimensions containing individual channels that are tapered. Potentially, a wide range of materials are available for the film and the low adhesion layer which together form the confining "walls" of the channels. Channel networks can thereby be assembled from materials with elastic moduli and imperviousness characteristic of metals and ceramics as opposed to the soft materials currently used in fabricating most microfluidic channels. Moreover, the properties of these materials can be selected for compatibility with specific chemical or biological environments. Filters and sieves formed as channel sequences having different cross-sections for sorting submicron particles in a fluid are potential applications. Further exploratory efforts are underway to study the potential of networks with Y-junctions, telephone cords and zigzags as nanoscale mixers.

References

[1] J.W. Hutchinson, Z. Suo: Adv. Appl. Mech. 29 (1992) 63.
[2] H.M. Jensen: Acta Metal. Mater. 41 (1993) 601.
[3] B. Audoly: Phys. Rev. Lett. 83 (1999) 4124.
[4] M.-W. Moon, H.M. Jensen, K.H. Oh, J.W. Hutchinson, A.G. Evans: J. Mech. Phys. Solids 50 (2002) 2355.
[5] L.B. Freund, S. Suresh: Thin film materials: Stress, defect formation and surface evolution, Cambridge Univ. Press, Cambridge (2004).
[6] A. Lee, B.M. Clemens, W.D. Nix: Acta Mater. 52 (2004) 2081.
[7] J.P. McDonald, V.R. Mistry, K.E. Ray, S.M. Yalisove: Appl. Phys. Lett. 88 (2006), 183113.
[8] M.-W. Moon, K.-R. Lee, K.H. Oh, J.W. Hutchinson: Acta Mater. 52 (2004) 3151.
[9] K. Gutensohn, C. Beythien, J. Bau, T. Fenner, P. Grewe, R. Koester, K. Padmanaban, P. Kuehnl: Thromb. Res. 99 (2000) 577.
[10] W.J. Ma, A.J. Ruys, R.S. Mason, P.J. Martin, A. Bendavid, Z.W. Liu, M. Ionescu, H. Zreiqat:. Biomaterials 28 (2007) 1620.
[11] R.J. Narayan, P.N. Kumta, C. Sfeir, D.H. Lee, D. Olton, D.W. Choi: JOM 56 (2004) 38.

[12] M. Mrksich, L.E. Dike, J. Tien, D.E. Ingber, G.M. Whitesides: Exp. Cell Res. 235 (1997) 305.

[13] J.P. Bearinger, S. Terrettaz, R. Michel, N. Tirelli, H. Vogel, M. Textor, J.A. Hubbell: Nature Mater. 2 (2003) 259.

[14] P.J.A. Kenis, R.F. Ismagilov, G.M. Whitesides: Science 285 (1999) 83.

[15] G.M. Whitesides, E. Ostuni, S. Takayama, X.Y. Jiang, D.E. Ingber: Annu. Rev. Biomed. Eng. 3 (2001) 335.

[16] J.C. McDonald, D.C. Duffy, J.R. Anderson, D.T. Chiu, H.K. Wu, O.J.A. Schueller, G.M. Whitesides: Electrophoresis 21 (2000) 27.

[17] H.P. Chou, C. Spence, A. Scherer, S. Quake: Proc. Natl Acad. Sci. USA 96 (1999) 11.

[18] H.-H. Yu, J.W. Hutchinson: Int. J. Fract. 113 (2002) 39.

[19] M.-W. Moon, J.-W. Chung, K.-R. Lee, K.H. Oh, R. Wang, A.G. Evans: Acta Mater. 50 (2002) 1219.

[20] N.R. Tas, P. Mela, T. Kramer, J.W. Berenschot, A. van den Berg: Nano Lett. 3 (2003) 1537.

[21] N.R. Tas, J. Haneveld, H.V. Jansen, M. Elwenspoek, A. van den Berg: Appl. Phys. Lett. 85 (2004) 3274.

[22] L.J. Yang, T.J. Yao, Y.C. Tai: J. Micromech. Microeng. 14 (2004) 220.

[23] N. Ichikawa, K. Hosokawa, R. Maeda: J. Colloid Interf. Sci. 280 (2004) 155.

[24] R.S. Butter, D.R. Waterman, A.H. Lettington, R.T. Ramos, E.J. Fordham: Thin Solid Films 311 (1997) 107.

[25] M. Schneegans, E. Menzel: J. Colloid Interf. Sci. 88 (1982) 97.

[26] C.D. Bain, J. Evall, G.M. Whitesides: J. Am. Chem. Soc. 111 (1989) 321.

[27] A.D. Stroock, S.K.W. Dertinger, A. Ajdari, I. Mezic, H.A. Stone, G.M. Whitesides: Science 295 (2002) 647.

[28] H.A. Stone, A.D. Stroock, A. Ajdari: Ann. Rev. Fluid Mech. 36 (2004) 381.

[29] H. Daiguji, P.D. Yang, A. Majumdar: Nano Lett. 4 (2004) 137.

[30] V.R. Dukkipati, J.H. Kim, S.W. Pang, R.G. Larson: Nano Lett. 6 (2006) 2499.

Correspondence address

Professor J. W. Hutchinson
School of Engineering and Applied Sciences, Harvard University
29 Oxford St., Cambridge, MA 02138 USA
Tel.: +1 617 495 2848
Fax: +1 617 496 0601
E-mail: Hutchinson@husm.harvard.edu